

Universität Heidelberg  
Institut für Informatik  
Engineering Mathematics

Bachelor-Thesis

Continuous Modeling of Extracellular  
Matrix Invasion by Tumor Growth

Name: Maximilian Bing

Matrikelnummer: 3606060

Betreuer: Professor Vincent Heuveline

Datum der Abgabe: April 2, 2024

Hiermit versichere ich, dass ich die Arbeit selbst verfasst und keine anderen als die angegebenen Quellen und Hilfsmittel benutzt und wörtlich oder inhaltlich aus fremden Werken Übernommenes als fremd kenntlich gemacht habe. Ferner versichere ich, dass die übermittelte elektronische Version in Inhalt und Wortlaut mit der gedruckten Version meiner Arbeit vollständig übereinstimmt. Ich bin einverstanden, dass diese elektronische Fassung universitätsintern anhand einer Plagiatssoftware auf Plagiate überprüft wird.

---

Abgabedatum:

## Zusammenfassung

Krebszellen können sich vom Primärtumor lösen und das umgebende Gewebe abbauen. Kontinuierliche mathematische Modelle wurden in der Vergangenheit mehrmals verwendet, um diesen Prozess besser zu verstehen. In diesem Zusammenhang basiert das Modell in der Regel auf mindestens drei Schlüsselkomponenten: den Tumorzellen, dem umgebenden Gewebe oder der extrazellulären Matrix (ECM) und den matrixabbauenden Enzymen (MDE). Das hier verwendete Modell beschreibt die obigen drei genannten Parameter, wobei Nullstrom Randbedingungen verwendet werden.

Die Analyse dieses Modells wird in der Literatur größtenteils in  $1D$  durchgeführt, und einzelne Beispiele wurden in  $2D$  gemacht. Allerdings zeigen vorläufige Reproduktionen des Modells, dass höhere Dimensionen signifikant unterschiedliche Ergebnisse liefern. Daher stellt sich die Frage, ob die Parameter für dieses Modell für Simulationen in  $2D$  oder  $3D$  unterschiedlich ausgewählt werden müssen oder ob die Ergebnisse und Analysen für den eindimensionalen Fall inkorrekt sind.

Darüber hinaus wurde in der Literatur die heterogene Struktur der extrazellulären Matrix (ECM) bereits behandelt. Die Struktur der epithelialen Schicht und der benachbarten extrazellulären Matrix ist jedoch in biologischem Gewebe organisierter als in den gezeigten Simulationen und anderen Beispielen. Daher könnten einfachere Unterteilungen der Geometrie in ECM-Gewebe aussagekräftigere Ergebnisse liefern.

Das Ziel dieser Arbeit ist es, einerseits die Parameter und das Modell für höhere Dimensionen zu untersuchen und andererseits eine einfache Heterogenität der ECM-Struktur in Betracht zu ziehen.

# Abstract

Cancer cells can migrate from the primary tumor and degrade the surrounding tissue. Continuous mathematical models have been used several times in the past to better understand this process. In this context, the model is usually based on at least three key species, the tumor cells, the surrounding tissue or extracellular matrix (ECM) and the matrix degradative enzymes (MDE). The investigated model in this work describes the above mentioned 3 parameters, with zero-flux boundary conditions.

The analysis of this models is mostly done in  $1D$  in the literature and individual examples were done in  $2D$ . However, reproductions of the model show that higher dimensions produce significantly different results. The question therefore arises as to whether the parameters for this model need to be selected differently for simulations in  $2D$  or  $3D$ , or whether the results and analysis for the one dimensional case is incorrect.

Ergebnis einfuegen

Furthermore, the heterogeneous ECM structure has been addressed in the literature. However, the structure of the epithelial layer and the adjacent extracellular matrix is more organized in biological tissue than in the simulations shown in and, for example. Therefore, simpler subdivisions of the geometry into ECM tissue could provide more meaningful results.

The aim of this work is to investigate the parameters and the model for higher dimensions on the one hand, and to consider a simple heterogeneity of the ECM structure on the other hand.

# Contents

<b>1</b>	<b>Introduction</b>	<b>5</b>
<b>2</b>	<b>Theoretical Basics</b>	<b>6</b>
2.1	Basics of Tumor Biology . . . . .	6
2.2	Mathematical Methods in Oncology . . . . .	7
<b>3</b>	<b>Modelling</b>	<b>8</b>
3.1	Mathematical Formulation . . . . .	8
3.2	Numerical Model and Parameters . . . . .	9
<b>4</b>	<b>Method</b>	<b>12</b>
<b>5</b>	<b>Experiments and Results</b>	<b>14</b>
5.1	Two dimensional Results without Proliferation . . . . .	14
5.1.1	Replicating results . . . . .	14
5.1.2	Parameter Analysis . . . . .	17
5.2	Two dimensional Results with Proliferation . . . . .	27
5.3	Three Dimensional Results . . . . .	27
5.3.1	Replicating Results . . . . .	27
5.3.2	Parameter Analysis . . . . .	27
5.4	Three Dimensional Simulations with Heterogenous ECM Structure . . . . .	27
<b>6</b>	<b>Conclusion and Discussion</b>	<b>30</b>
6.1	Extra-Dimension Evaluation . . . . .	30
6.2	Inter-Dimension Evaluation . . . . .	30

# 1 Introduction

Modelling tumor growth plays a key role in understanding the complex mechanisms, governing development and progression of cancer diseases. Since cancer is one of the leading death causes worldwide and many of its forms are incurable, challenges in the area of Oncology require researchers to have a deep understanding in as well the biological foundation, which lead to malignant cell mutation and factors for tumor growing and spreading, as well as the mathematical models used for simulating these events. This Bachelorthesis is dedicated to analyse Anderson et al.'s [1, 2] model for tumor modelling. The dynamics of tumorous growth are an intricate system, which is influenced by numerous biological and chemical factors, as well as genetic pre-dispositions, the surrounding tissue of cancer cells, angiogene processes and interactions with the immune system. The integration of these factors in mathematical models allow us to decode these complex interactions with quantification and help us understand the fundamental mechanisms, which surround cancerous diseases, as the last year's experience has shown.

Mathematical models are a very important part in Oncology. They are used to quantify biological phenomena and therefore help to predict and understand tumor development and treatment response. In Mathematical Oncology we differentiate between continuous, discrete and hybrid models. For the continuous type, cells and tissue are described over time with differential equations modelling continuous quantities like in our case the cell or extracellular matrix density. In the discrete case, a entity based model is used, pursued with the goal to better understand the phenomena on cell level. This approach allows the researcher to better implement biological effects a cell has with its outer circumstances, like interaction with other cells, nutrients or other microorganisms. As the name implies do these models use discrete values to describe the temporal course of events. Hybrid models try to combine both approaches, to offer efficient systems capturing cell level events as well as continuous changes in outer circumstances.

In this work we are investigating how a continuous model proposed by Anderson et al. [1, 2] to analyse tumor development in the early stages performs in the case of different dimensions and free parameter values. The model examines the first two stages of a cancer disease; tumor initiation, where the tumor cells are localized to a small area and have not yet spread throughout the body; and tumor promotion, with the tumor cells growing and proliferating, invading the surrounding tissue. From examples of the original paper we can already see that the model's results vary with the dimensionality of the space we are modelling the partial differential equations in. Our main focus lies on comparing simulations of two dimensions with those of three dimensions of extracellular matrix invasion by the tumor growth. Additionally to the variation of dimensions we will have a closer look on how the geometry of the extracellular matrix will influence the tumor development.

Another point of interest is the investigation of how the model's free parameters influence the tumor dynamics growth. An important task is to give those parameters a biological meaning and to eventually gain insight to how to adjust them to make the simulation more realistic.

## 2 Theoretical Basics

### 2.1 Basics of Tumor Biology

The body of a living creature is made up of more than 200 different types of cells, the coordination between the cells and their surroundings keep the body running. Each of these cells is built from the genetic information encoded in the DNA, located in the cells' nuclei. Though the nucleotide sequence of DNA is well checked and maintained throughout the cell's life, mutations still occur that cause the changes in the DNA of a cell. These mutations may be of a positive, negative or neutral nature. In the case of a negative mutation this alternation of the DNA may cause diseases, with cancer being one of them. The failure of the complex system managing cell birth, proliferation, and cell death (apoptosis) causes cancer, resulting in an uncontrolled cell proliferation in a at first local area. An conglomeration of cancer cells is called a tumor.

A cancer disease typically follows five stages. First the tumor initiation phase where it comes to the above explained genetic mutations of normal cells. The next stage is the tumor promotion stage, in which the mutated cells of phase one may experience further genetic alterations, with the result of uncontrolled growth and proliferation of the cancerous cells. The third stage is the tumor progression stage, where the cancerous cells progress in growing and proliferating, reaching a critical mass, they form a tumor at a local site of the body. Fourth comes the invasion stage, here the tumor is able to invade surrounding tissue and enter the blood circulation system or the lymphatic system. Next the tumor cells which have invaded the blood circulation of lymphatic system spread throughout the body and form new tumors. This stage is called Metastization. To further grow the tumors need to have access to nutrient and oxygen supply. During angiogenesis a tumor develops blood vessels of its own securing its nutritional provision. At this stage first symptoms of host may appear, enabling medical treatment.

In our model the focus lies on the first two stages; tumor invasion and tumor progression, so we are going to have a deeper look at those two phases. The tumor invasion stage is characterized by the malignant cells gaining the ability to penetrate and invade the surrounding tissue. The tumor cells break through the normal tissue barrier and infiltrate neighboring structures. In order to do so the cancer cells produce so called matrix-degrading enzymes which break down the extracellular-matrix. This not only helps local spreading but also destroys otherwise healthy tissue and cells in the affected area. In the next phase the tumor progression stage, the tumor has grown larger and the cancerous cells take on more aggressive behaviour, by invading the surrounding area further. Whilst they keep growing uncontrolled they are also affected by further genetic instabilities, which lead to more mutations among the tumor cells, resulting possibly in the development of resistant cancer cells. Already in this stage the affected area is exposed to heavy tissue damage and functional disabilities.

The most important factors influencing those two phases are the genetic dispositions of the tumor cells towards proliferation and the evasion of apoptosis, which increase the invasive potential. Another important factor is geometry of the extracellular matrix, as well as the exact macromolecules which make it up. A strong immune biological defense reaction also helps the body defend against the spreading of the cancer cells, so evasion

of detection and destruction of the tumor cells plays a key role for the first stages. To invade the affected area the malignant cells need to be able to move freely and fastly. In order to do so cancer cells can gain the ability to lose adhesion properties which healthy cells have, to allow migrating into surrounding tissue.

## 2.2 Mathematical Methods in Oncology

Mathematical Methods and Models in Oncology play a crucial role in analysing, understanding and predicting cancer development. Since the objective of this research underlies complex and intricate biological systems and mechanisms, there exist many models, which find their respective application in many distinct areas of this research field. These methods can be coarsely divided into three sections; continuous, discrete and hybrid models. For describing tumor growth, exponential and logistic growth models are often used, the later allowing limiting factors to play a role during modelling. These methods are a subclass of the differential equations approach which base their functionality on a ordinary or partial differential equation, studying the continuous approach. Like in our model they are not limited to consist of one equation but can of many, therefore also incorporating limiting or accelerating factors. These models in general deal with continuous parameters like densities, or fluid concentrations, for example spacial and temporal nutritional supply or drug concentration, as well as their effects on the affected area over time. Discrete models use a agent-based approach, where the participating individual entities are modeled as objects which can interact on their environment, this means for example cell-cell interaction or cell-tissue interaction. This enables researchers to focus on biological effects during modelling. With these approaches we can also simulate genetic and evolutionary events. For example studying the genetic alternations of tumor cells.

Hybrid models combine both aforementioned methods, of using continuous and discrete models. Like in the model proposed by Franssen et al. [3], these approaches allow to incorporate the exactness of continuous models with the wide range of biological effects of discrete models.

But not all models try to model tumor growth, there are others concerning for example optimality regarding drug dosages or radiation exposition, offering personalized treatment, or Machine Learning and Data Mining methods analysing large datasets, to identify patterns and predict outcomes. The later method may be used in all kinds of applications, for example spacial or temporal cancer development but also for drug dosage optimization for individual patients. Putting all these methods together gives us a powerful toolbox to simulate and understand cancer biology. Like the last years have shown they are applied in a wide range, offering insight for all areas of cancer research. Therefore it is important not only to come up with methods but to also evaluate their usefulness and meaningfulness regarding different areas of research.



## 3 Modelling

### 3.1 Mathematical Formulation

The model proposed by Anderson et al. [1, 2] and Chaplain et al. [1, 3, 4], extended with terms for cell modelling cell proliferation consists of a system of linearly coupled partial differential equations:

$$\frac{\partial c}{\partial t} = D_c \Delta c - \chi \nabla \cdot (c \nabla e) + \mu_1 c \left( 1 - \frac{c}{c_0} - \frac{e}{e_0} \right) \quad (1)$$

$$\frac{\partial e}{\partial t} = -\delta m e + \mu_2 c \left( 1 - \frac{c}{c_0} - \frac{e}{e_0} \right) \quad (2)$$

$$\frac{\partial m}{\partial t} = D_m \Delta c + \mu_3 c - \lambda m \quad (3)$$

with zero-flux boundary conditions,

$$n \cdot (-D_c \nabla c + c \chi \nabla e) = 0 \quad (4)$$

$$n \cdot (-D_m \nabla m) = 0 \quad (5)$$

where the free parameters are  $D_c$ ,  $D_m$ ,  $\chi$ ,  $\delta$ ,  $\mu_1$ ,  $\mu_2$ ,  $\mu_3$  and  $\lambda$ .

The variable  $c$  describes the tumor cell density,  $e$  the density of the extracellular matrix and  $m$  the matrix-degrading enzyme concentration. All of those functions are mathematically defined to be mapping a 1,2 or 3 dimensional spacial value and a point in time to a scalar value describing the concentration at a specific point in space and time,  $\{c, e, m\} : \mathbb{R}^3 \times \mathbb{R} \rightarrow \mathbb{R}$ .

To derive at the expression for the tumor cell concentration  $c$  we are going to assume that the tumor cell's movement is subject to two influences, haptotaxis and random movement. Haptotaxis is a directed migratory response of cells to gradients of fixed or bound chemicals [1] and random movement is influenced by for example mechanical stress, electric voltage or other such physical effects. To get an expression for how much or how fast the tumor cells move, we need to define what flux is, flux is defined to be the amount of a substance which crosses a unit area in unit time. Incorporating the two assumed influencing factors into our mathematical model we define the haptotactic flux  $J_{hapto} = \chi c \nabla e$ , where  $\chi$  is the haptotactic flux coefficient, and the random flux  $J_{random} = -D_c \nabla c$ , where  $D_c$  is random mobility constant. In general this parameter could also be a function of both extracellular matrix and matrix-degrading enzyme concentration  $D_c \rightarrow D(e, m)$ . As we know cells proliferate and grow over time, so we want to respect this in our model with a term for tumor cell proliferation:  $\mu_1 c (1 - \frac{c}{c_0} - \frac{e}{e_0})$ . The idea is that this term describes the cell proliferation with a logistic growth model,  $\mu_1$  describing the proliferation rate. In the initial model proposed by Anderson et al. [1, 2] and Chaplain et al. [1, 3–5], they did not respect proliferation of tumor cells and extracellular matrix and therefore applied a conservation equation for the tumor cells  $\frac{\partial c}{\partial t} + \nabla \cdot (J_{hapto} + J_{random}) = 0$ , in our model we extend this conservation formula with a proliferation rate. Explicitly inserting the flux formulas and logistic growth function for the tumor cells gives us:  $\frac{\partial c}{\partial t} + \nabla \cdot (J_{hapto} + J_{random}) + \mu_1 c (1 - \frac{c}{c_0} - \frac{e}{e_0}) = \frac{\partial c}{\partial t} + \chi \nabla \cdot (c \nabla e) - D_c \Delta c + \mu_1 c (1 - \frac{c}{c_0} - \frac{e}{e_0})$ .

Which is equivalent to equation 1.

To model the extracellular-matrix concentration  $e$ , we assume that the enzymes degrade the extracellular matrix upon contact. This assumption is simply modeled by the equation  $\frac{\partial e}{\partial t} = -\delta m e$ ,  $\delta$  is a positive constant describing this annihilation process. To this we also add a term describing the proliferation process:  $\frac{\partial e}{\partial t} = -\delta m e + \mu_2 c (1 - \frac{c}{c_0} - \frac{e}{e_0})$ . Modelling the matrix-degrading enzyme concentration  $m$ , we combine a diffusion term with production and decay terms. The diffusion term is described like in tumor cell concentration, with the addition that haptotactic fluxes are neglected and only random mobility is assumed,  $J_{random} = -D_m \nabla m$ . The production term depends on the tumor cell concentration and the decay term on the extracellular matrix concentration. This results in the term:  $\frac{\partial m}{\partial t} = \nabla J_{random} + \mu c - \lambda e = D_m \Delta m + \mu_3 c - \lambda m$ ,  $\mu$  and  $\delta$  describing production and decay rates.

### 3.2 Numerical Model and Parameters

To make solving the model easier we are first going to non-dimensionalise all the equations 1 to 5 in a standard way, with the goal to rescale the space domain onto unit size. For one space dimension this results in the unit interval  $[0, 1]$ , for two dimensions the unit square  $[0, 1] \times [0, 1]$  and for three dimensions the unit cube  $[0, 1] \times [0, 1] \times [0, 1]$ . We start with rescaling the distance with an appropriate length scale  $L$  and the time with  $\tau = \frac{L^2}{D}$  ( $D$  being a chemical diffusion coefficient). The three variables are being rescaled with their initial values respectively  $c_0, e_0, m_0$ , which gives us this:

$$\tilde{c} = \frac{c}{c_0}; \tilde{e} = \frac{e}{e_0}; \tilde{m} = \frac{m}{m_0}$$

Next we modify the system's free parameters  $D_c, \chi, \delta, D_m, \mu_3, \lambda$ :

$$d_c = \frac{D_c}{D}, \quad \gamma = \chi \frac{e_0}{D}, \quad \eta = \tau m_0 \delta, \quad d_m = \frac{D_m}{D}, \quad \alpha = \tau \mu_3 \frac{c_0}{m_0}, \quad \beta = \tau \lambda.$$

with  $D$  being a reference chemical diffusion coefficient.

These modifications make the new system of coupled partial differential equations, where the tildes are dropped for simplicity's sake:

$$\frac{\partial c}{\partial t} = d_c \Delta c - \gamma \nabla \cdot (c \nabla e) + \mu_1 c \left( 1 - \frac{c}{c_0} - \frac{e}{e_0} \right) \quad (6)$$

$$\frac{\partial e}{\partial t} = -\eta m e + \mu_2 e \left( 1 - \frac{c}{c_0} - \frac{e}{e_0} \right) \quad (7)$$

$$\frac{\partial m}{\partial t} = d_m \Delta c + \alpha c - \beta m \quad (8)$$

with also updated zero-flux boundary conditions,

$$\zeta \cdot (-d_c \nabla c + c \gamma \nabla e) = 0 \quad (9)$$

$$\zeta \cdot (-d_m \nabla m) = 0 \quad (10)$$

where  $\zeta$  is an appropriate outward unit normal vector.

In order to use the finite element method we will change to the variational formulation.

If we assume each species to be in the Hilbert space  $H^1(\Omega)$ , the variational formulation can be derived by multiplying with a test function, integrating over the domain  $\Omega$  and use integration by parts and the Gauss theorem. This will give us a broader solution space and reduces the requirements of the solution regarding differentiability. With  $(\cdot, \cdot)$  denoting the  $L^2$ -scalar product on  $\Omega$  the following equation system results

$$\left(\frac{\partial c}{\partial t}, \varphi_c\right) = -D_c(\nabla c, \nabla \varphi_c) + \chi(c \nabla e, \nabla \varphi_c) + \mu_1 \left(c \cdot \left(1 - \frac{c}{c_0} - \frac{e}{e_0}\right), \varphi_c\right) \quad (11)$$

$$\left(\frac{\partial e}{\partial t}, \varphi_e\right) = -\delta(m e, \varphi_e) + \mu_2 \left(e \left(1 - \frac{c}{c_0} - \frac{e}{e_0}\right), \varphi_e\right) \quad (12)$$

$$\left(\frac{\partial m}{\partial t}, \varphi_m\right) = -D_m(\nabla m, \nabla \varphi_m) + \mu_e(c, \varphi_m) - \lambda(m, \varphi_m) \quad (13)$$

For the initial conditions we will assume that at dimensionless time  $\tau = 0$ , there is already a nodule of cells present centered around the origin in every dimension. For example in one dimension  $c$  is having the initial density distribution,  $c(x, 0) = \begin{cases} \exp(\frac{-x^2}{\epsilon}), & x \in [-0.25, 0.25] \\ 0, & x \notin [-0.25, 0.25] \end{cases}$ , with  $\epsilon$  being a positive constant. The tumor will have degraded some of its surrounding tissue in every experiment and hence we take the initial profile of the extracellular matrix to be  $e(x, 0) = 1 - 0.5c(x, 0)$ . At last we assume the initial matrix-degrading enzyme concentration to be proportional to the initial tumor cell density and therefore take  $m(x, 0) = 0.5c(x, 0)$ . These initial values are displayed in figure 3.2.

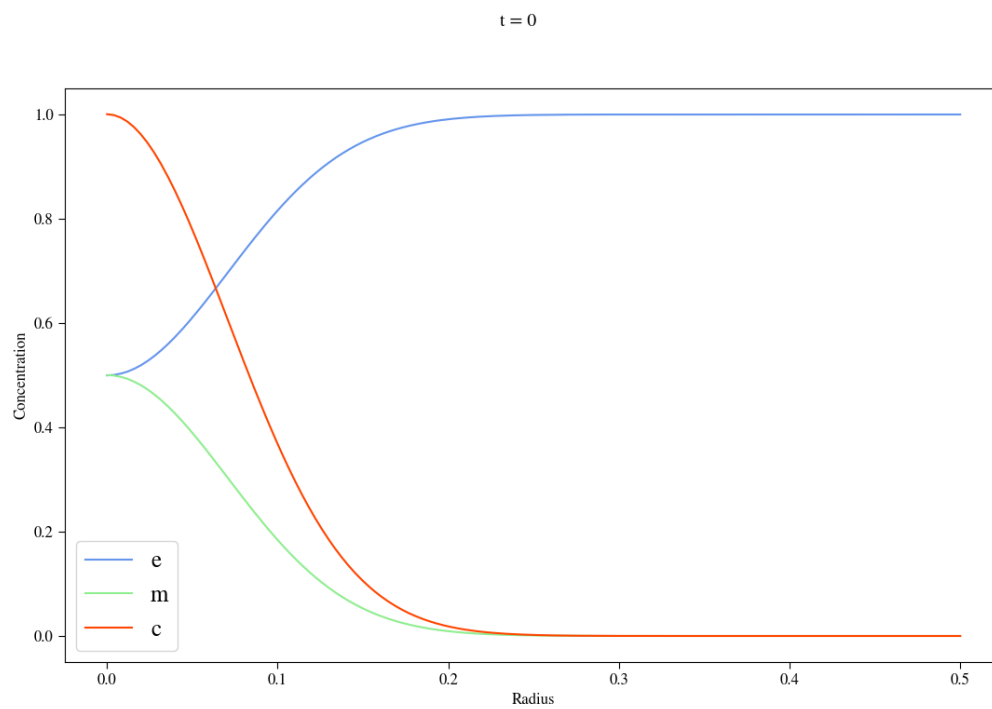


Figure 1: Visualization of the initial value distribution for an experiment in two space dimensions, radially symmetrical

## 4 Method

This work will investigate how the free parameters of the model given by the equations 6 - 10 will affect the spatial temporal progress of the numerical simulation. For the numerical simulation we will use the weak form given with equations 11 - 13 and solve it using HiFlow. To study the results of the numerical simulation ParaView is used, producing informative plots to compare the evolution of the simulation in time. For this we rely on the tool Plot Over Line to give radially symmetrical results of the three variables of tumour and extracellular matrix density and matrix-degrading enzymes, an example for this can be seen in figure 3.2 showing the initial conditions. In figure 2 you can see the configuration for the Plot Over Line tool, since we are considering the experiments on the unit square in 2D dimensional case, the line starts at  $x = 0.5, y = 0.5$  and ends at  $x = 0.5, y = 1$ .

For the three dimensional experiments a different tool was used ....*explain 3D experiments methodology*

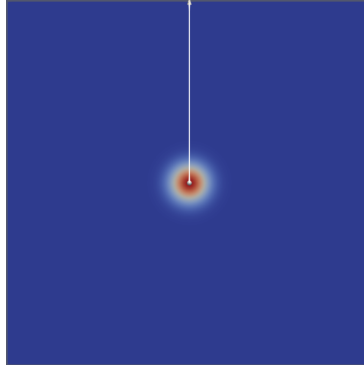


Figure 2: Plot Over Line Tool Configuration

All experiments that consider the ECM to be homogenous start with the same initial values as seen in figure 3.2. Experiments observing the effects of a heterogeneous ECM use different initial values, like seen in *initial values heterogeneous ECM*

This work starts with *trying to replicate/replicating* numerical simulations done by other papers. Since there were only 1D simulations done previously, the model will be adjusted in such a way, that the Plot Over Line graphs mimic the plots given by the previous experiments. This will serve two purposes, first and minor it will verify a correct implementation of the model and second this will give us a starting point by which we can vary the parameters, investigating the phenomena this model exhibits.

We will start with examining 2D experiments with homogenous ECMs, using our model with the parameters  $\mu_1$  and  $\mu_2$  both set to zero, considering a case with no proliferation, after this we will introduce proliferation, varying also  $\mu_1$  and  $\mu_2$ . The same will be done for the 3D cases, also at first neglecting proliferation to apply it in a later stage. Our focus here lies on investigating the effects of the parameters, but also on how the dimension changes results, with fixed free parameters. At last we will have a brief outlook on how a heterogeneous ECM influences our results

The results of the above experiments will be summarized and discussed in the Conclusion and Discussion part, pointing out the important characteristics of the simulations and discussing the sensitivity of each of the parameters and the influence of the dimension.

At this point we will have an outlook on how to extend the model with more continuous and or discrete adaptations.

Looking at the parameter estimates from [2] to non-dimensionalise the time, we see that with  $L \in [0.1cm, 1cm]$  and  $D \approx 10^{-6} \frac{cm^2}{s}$ ,  $\tau = \frac{L^2}{D}$  gives a relative big temporal range,  $\tau_{min} = 1000s = 16.66min$  and  $\tau_{max} = 1000000s = 16666.66min$ , which makes it hard, to find the correct time step value to compare our simulation results with the one from [2] and [6]. Another challenge are the diffusion coefficients, since they are dependent on the dimension we are in, we have to find our own estimate as a baseline value. For our experiments we will use a set of baseline parameters, which will be evaluated experimentally, and from there vary one parameter at a time to get a overview of their effects and later we will incorporate variation of multiple paramters in accordance with the numerical model.

## 5 Experiments and Results

For all the plots of the experiments the red curve indicates the tumour cell density, the blue curve the ECM density and the green curve the MDE concentration. In all of the experiments we used the value of  $\epsilon = 0.01$  to match the initial conditions from [2] and [6]. Mathematical Intuition of the three curves and how the parameters interact.

### 5.1 Two dimensional Results without Proliferation

#### 5.1.1 Replicating results

We will start with replicating the experiment from Anderson et al.[2], Figure 3, trzing to make our curves fit the findings in their diagrams.

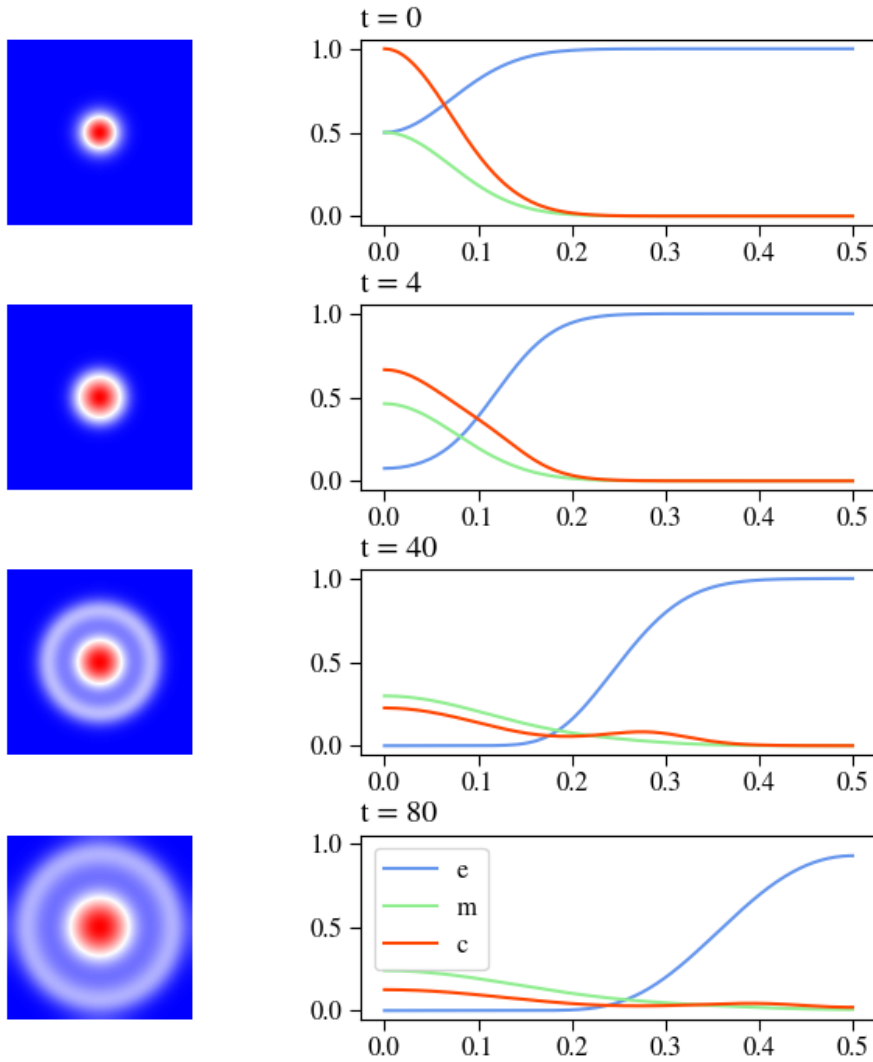


Figure 3: Images on left side 2D plots of the experiment, images on right side results produced by applying plot over line tool

We therefore used the same parameters as in Anderson et al.'s first one dimensional experiment with the values;  $d_c = 0.001, d_m = 0.001, \gamma = 0.005, \eta = 10, \alpha = 0.1, \beta = 0, \mu_1 = 0, \mu_2 = 0$ . Figure 3 shows these results for four different points in time. Since our experiments are performed in two dimensions you can see on the left side the two dimensional plots of the tumour cell density and on the right side you can see plots produced by applying the Plot Over Line tool configured like described in the method section, where there is not only the tumour cell density visible but also the matrix decaying enzyme concentration and the extra cellular matrix concentration. We choose these points in time, because we used a different timescale than Anderson et al. and as you will later see, our time points capture the effects that can be observed studying their results quite well, which implies that for every time step Anderson et al. did we had to do 4. The problem with the two dimensional plots is that as you can see overlazing the different variables of tumour cell density, MDE concentration and ECM concentration, makes the plots unreadable, so you can only show one at a time, additionally to this it is not possible to estimate values for  $c, e, m$  at different locations in space and time. These problems are solved using the plot over line tool, as you can see in the plots on the right side the curves for  $c, e, m$  are clearly distinguishable and we can estimate their values at locations. This is why for most experiments we resort to using the plot over line plots instead of full 2D simulation images, they make evaluating and comparing the respective experiments way easier and still capture for the most part all occurring effects. Starting from the initial values at  $t = 0$  we see that after four time steps a very small unevenness has formed for the tumour cell density at  $x \approx 0.1$ . Diffusion and Haptotaxis have stretched the curve for the tumour cells as did diffusion for the MDEs. The ECM has clearly been decayed at the origin. The next image shows the simulation after 40 timesteps; we see that the unevenness of the tumour cell concentration of the previous point in time has been propagated to form a small hill at the leading edge of the tumour cells invading the surrounding tissue, at  $x \approx 0.28$ , this effect is due to the haptotactic influence, which pulls the tumour cells further into the accessible area towards the gradient of  $c$  grad  $e$ , creating a separation for the tumour cell density, where the other part is still oriented towards the origin. MDEs also continued their diffusion into the area, decaying the ECM in their wake, decreasing them further. In the last image, after 80 simulation time steps, we see that as well the hill that has formed at the leading edge of the tumour cells as well as the concentration of tumour cells at the origin, have continued flattening and taking on a constant concentration throughout space, though we can still clearly distinguish both areas. If we were to look at the simulation at later points in time, this curve will flatten even more, since with more time the ECM will be decayed and therefore the haptotactic flux coefficient  $\gamma$  will lose its influence, leaving the movement of the cells to diffusion only. The curve for the MDEs has also flattened, yet not as strongly as the tumour cells concentration and as the observed before the ECM decayed where the MDEs were previously. They will continue to do so, decaying the ECM and their concentration over time will increase due to no limiting factors in this experiment and on-going production contributed by the tumour cells  $c$ .

Comparing 3 to figure 1 in [2], we can see major differences. The first image showing  $t = 0$  looks the same, which confirms that both experiments start with the same initial



values condition. In the images showing the simulation at the second time checkpoint we see that though the tumour concentration and ECM density values are approximately the same, the MDE concentration is slightly lower in our experiment, which will get more pregnant in the later images. The unevenness having formed at the leading edge of the tumour cell concentration also looks to be slightly smaller. The differences in the third image are more striking, both  $c$  and  $m$  have considerably lower concentrations, yet the ECM value looks to in line. In our case the diffusion of the tumour cells into the tissue also seems to happen a littel bit too fast. The last time checkpoints strengthens our findings, showing the same behaviour with ECM being approximately the same, tumour cell density and MDE concentration being clearly lower in our experiment and invasion of tissue happening too fast, leaving the lump at the origin  $x = 0$  too small.

This first of all confirms the initial supposition that with changing the dimension for the simulations the results also vary. We will now adjust the parameters iteratively to make the results using two dimensions mimick the results from Anderson et. al as closely as possible. For this we will start with varying the MDE production coefficient  $\alpha$ , to get higher concentration values, and also change the diffusion and haptotaxis terms of the tumour cells  $d_c$  and  $\gamma$ , to adjust the motility of the tumour cells and therefore also influence the invasion speed of them into the surrouding tissue.

Figure 4 shows a comparison of the parameters  $\alpha$ ,  $d_c$  and  $\gamma$  have on a specific curve. Comparing different values for  $\alpha$  and their effect on the curve of the MDE concentration, shows that, especially looking at the later points in time  $t = 4$  and  $t = 8$ , with values for  $\alpha$  between 0.3 and 0.4 we will get a good approximation. The values of the original paper for the MDEs are for  $t = 4$   $m(0) = 0.6$  and at  $t = 8$   $m(0) = 0.7$ . Fine tuning this parameter led us to  $\alpha = 0.35645$ .

Looking at  $d_c$  we chose a value of  $d_c = 5e - 4$ . Using higher values for this parameter will result in numerical instability and results that are not useable. For  $\gamma$  we made a slight adjustment upwards to  $\gamma = 0.0055$  to have a little bit more pull on the tumour cells outward, to match the invasion speed observed in the original paper. This yields results where the small hill at the leading edge of the tumour cell concentration in the latter two points in time is a higher values for  $x$ , yet not as steep as for example  $\gamma = 0.007$ .

These adjustments leave with the final configuration for replicating the system with the curves in figure 5.1.1 and the parameter settings also seen in the same figure. Slightly adjusting the haptotatic flux to  $\gamma = 0.0055$  yields the following results, seen in figure 5.1.1. comparing our final version with the original one we can see that in the second point in time, at  $t = 4$  in our case, the values of the three curves at the  $x = 0$  are nearly the same. In the original experiment the bump in the curve for the tumour concentration looks more pregnant, but this is only due to the fact, that this experiment was most likely done on the unit line, not the unit cube, it also seems that they have done a rescaling of the x-axis. The two later points in time confirm the similarity with having also nealy the same values for the three curves at  $x = 0$  but also their respective propagations in time look to be in line with the original experiment.

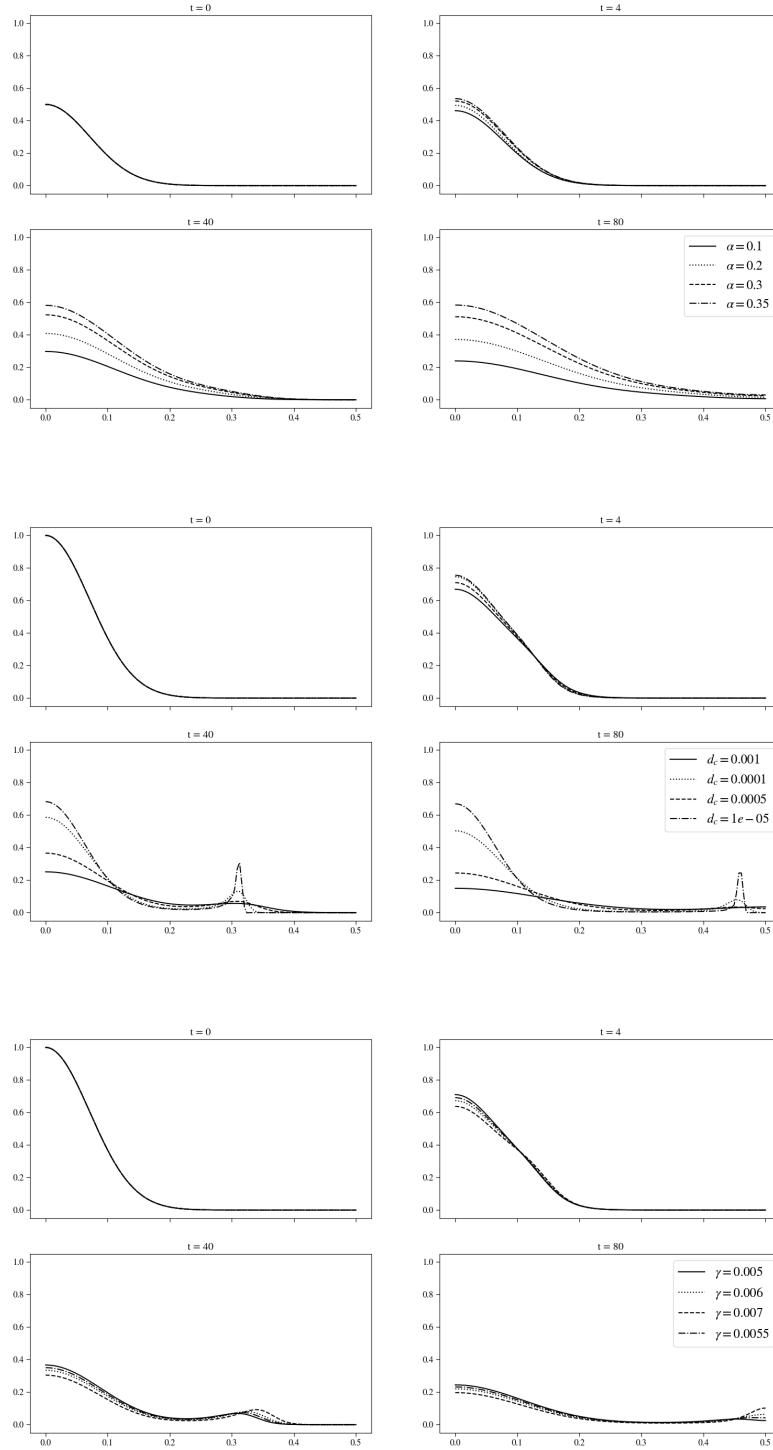
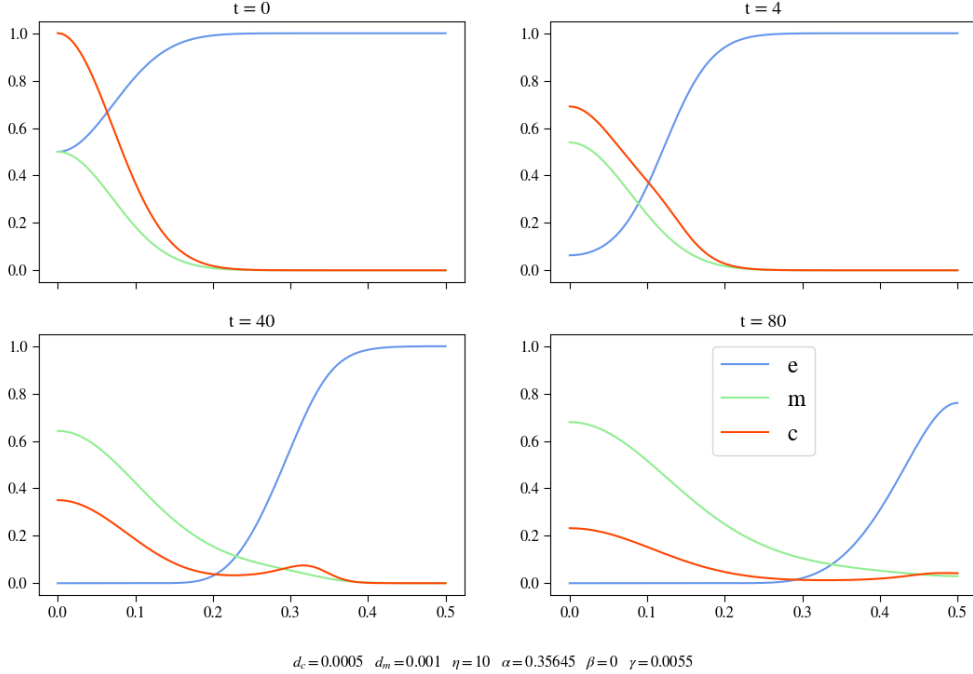


Figure 4: Caption

### 5.1.2 Parameter Analysis

From the replicated results shown in figures 5.1.1, we saw that if we variate certain parameters the results also vary strongly. Therefore we are now going to have a look at



how changing one parameter affects the output of the whole system. For this we assume the parameter values of the replicated results to be our set of baseline parameters, from there in each experiment only one parameter is changed.

### $d_c$ Variation

The parameter analysed in this section describes the diffusion of the tumour cells and is integrated into the equations as being dependent on the laplacian of the tumour cells  $\Delta c = (\frac{\partial^2 c}{\partial x^2} + \frac{\partial^2 c}{\partial y^2} + \frac{\partial^2 c}{\partial z^2})$ . Leaving out the proliferation term our equation for  $\frac{\partial c}{\partial t}$  also depends on  $\gamma$  a coefficient for the haptotactic flux. The mathematical intuition is that if we will decrease  $d_c$  we will see the effects of  $\gamma$  taking over the simulation results for the  $c$  curve, meaning that the tumour cells are more likely to drift outward and let themselves be pulled by the ECM concentration  $e$ , due to haptotaxis, leaving only a little concentration at the center  $x = 0$ , creating a bigger hill on the leading edge of the tumour concentration (below where  $c \nabla e$  will be highest). On the other hand if we increase  $d_c$  the effects of haptotaxis will diminish, the tumour cells will be subject to bigger diffusion pulling them more evenly into the tissue, there will be less of a leading hill being pulled outwards, since the diffusion will happen too fast, making this effect irrelevant. Looking at both experiments in figure 5, we can see these assumptions confirmed. The smaller  $d_c$  gets the higher the influence of  $\gamma$  will be and vice versa. Considering the red curves, the tumour cell density, after  $t = 4$  timesteps the dashed curve, describing  $d_c = 1e - 5$ , takes on a value a little higher than for the basecase of the solid curve with  $d_c = 5e - 4$  whilst the dotted curve, showing the results for  $d_c = 1e - 1$ , has already taken on a near constant

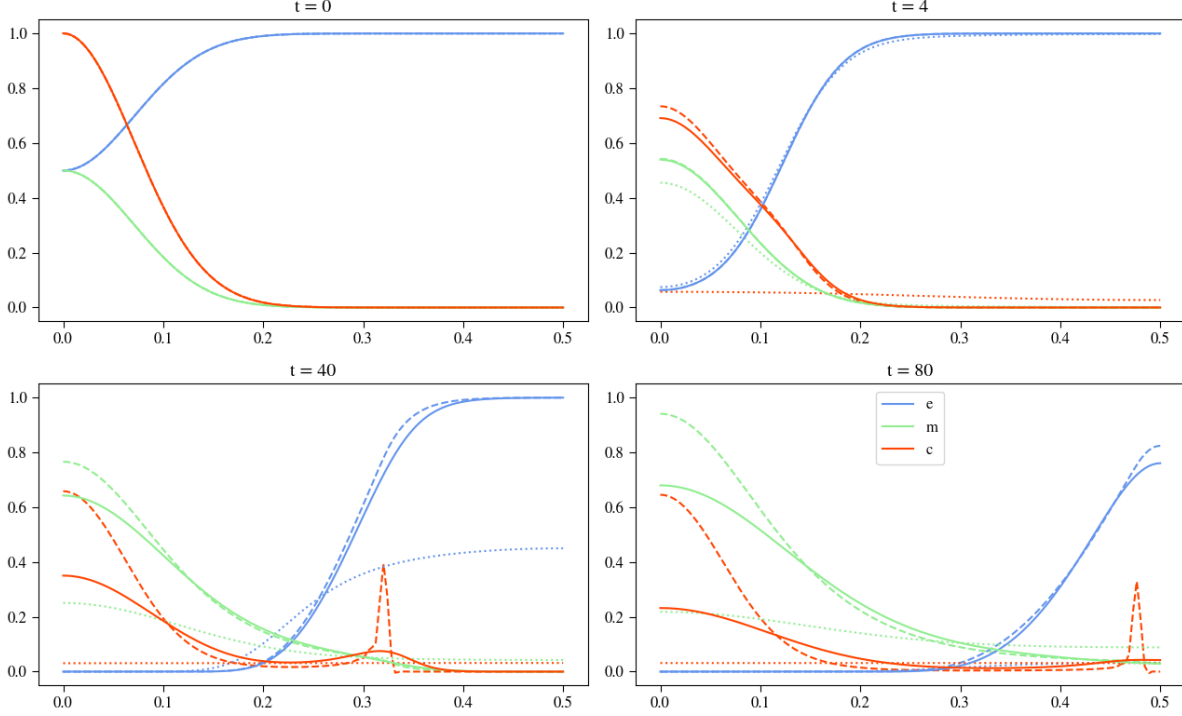


Figure 5: Plots show results for varying  $d_c$  whilst keeping the other parameters constant, in the images you can see the effects of  $d_c = 1e - 5$  in the dashed curve,  $d_c = 1e - 1$  in the dotted curve and  $d_c = 5e - 4$  in the solid line.

concentration throughout space. This shows that the higher the values for  $d_c$  are the faster the diffusion spreading throughout space will be, where for the solid and dashed line we can see small effects of haptotaxis in the second image, nothing of this is visible for the dotted line, where the diffusion effects completely cover up the effects of haptotaxis. For the MDE concentration we can observe that with rising values for  $d_c$  they also spread faster throughout space, this is first due to influence of the current  $c$  density on the motility of the MDEs and also due to the production term, meaning with faster spread throughout space we will get more even production of MDEs. The effect on the ECM concentration varying  $d_c$  seems to be little at stage. Looking at the next point time at  $t = 40$  we can see that the differences in the curves observed previously have intensified, with examining the tumour cell concentration, yielding now completely different results. The dotted curve has not visibly changed and while the solid curve describes the base case, we can see for the dashed curve that as above mentioned here the effects of haptotaxis, with a very pointy peak at the leading edge of the tumour cells. The other two curves differ also very visibly here, showing big variation MDE and ECM concentration. The MDEs diffuse faster throughout space the higher  $d_c$  is, with the dotted curve having flattened more than the other two, where the dashed curve has the highest concentration of MDEs at the origin still. This faster spreading of tumour cells and MDEs takes effect on the ECM, showing that the ECM for the dotted curve has clearly faster decayed than the other two, though for them we can see like for the MDEs visible differences considering degradation. In

the last image we can see another amplification of the previous mentioned effects, for the dotted curves,  $d_c = 1e - 1$ , they seem to have taken constant concentrations in space, except the green curve for the MDEs which is still higher around the origin than in outer regions, the red curve describing the tumour cells has again not changed staying constant and the ECM concentration has also been degraded towards zero every in space. The red dashed curve shows that the tumour cells density has two clear maxima in space one at the origin and one at the leading edge, whereas the solid curve is a lot more evenly distributed throughout space. Here you can also see that the red dashed curve takes on negative values, which indicate numerical instabilities, which will only increase decreasing  $d_c$ . These issues are due to the nature of the solver, where both factors influencing  $c$ ,  $d_c$  and  $\gamma$  need to be in a certain range to produce reasonable results, since negative values for the tumour cell density does not make any sense. The MDE concentration is as expected higher around the origin for the lower  $d_c$  values, this is due to the tumour cells also staying rather around the origin for this experiment and therefore producing more MDEs at this location in space. It is interesting to see that both effects of  $c$  and  $m$  comparing the dashed and solid curves seem to have little effect on the ECM concentration, but as we saw in the third image only a little concentration of MDEs is needed to efficiently decrease the ECM, this shows that the ECM degradation process happens so fast that minor differences in the MDE concentration have little effect on it and also as we can see that the major differences in the MDE curve are located around the origin, these differences seem to decrease with increasing distance. This comparison verifies that  $d_c$  has a rather impactful influence on the system, especially considering that the  $d_c$  values of the dashed and solid curves are only separated by a distance of  $5e5$ . Increasing  $d_c$  results in faster diffusion and also faster spreading throughout space, but also with faster degradation of the ECM and invasion of MDE of the area.

## $\gamma$ Variation

Inspecting the effects of  $\gamma$  we can assume the same as for  $d_c$  if we select higher values for  $\gamma$  the effects of haptotaxis, pulling the tumour cells into the tissue faster, leaving no cells at the origin, taking lower values for  $\gamma$ , the diffusion will be superior factor for the tumour cell motility, which will result in no secession at the leading edge of the tumour cells. The experiments, described in figure 6 verify the expected behaviour. After  $t = 4$  the solid and dashed red curves, indicating tumour concentration for the higher values for  $\gamma$ , have already built a lump that will in the later points in time form a secession, here we can already see that the dashed line with the highest value for  $\gamma$  has formed a larger lump than the curve for  $\gamma = 0.008$ . The tumour density curve for  $\gamma = 0.002$  does not show such behaviour. The curves for the MDE and ECM concentration still overlap at this point in time. The next image showing the simulation after  $t = 40$  timesteps shows that changing  $\gamma$  affects also the other curves. Whilst the tumour concentration for the values of 0.008 and 0.01 differ slightly by the amount of density that is left at the origin and the distance they have already invaded the surrounding tissue, the curve for the value  $\gamma = 0.002$  does not even show a leading edge here that is being pulled by haptotaxis into the tissue, yet it has the highest density at the origin for the  $c$  curves. We can also see that with increasing  $\gamma$  the invasion speed also increases. For the MDE curve we observe

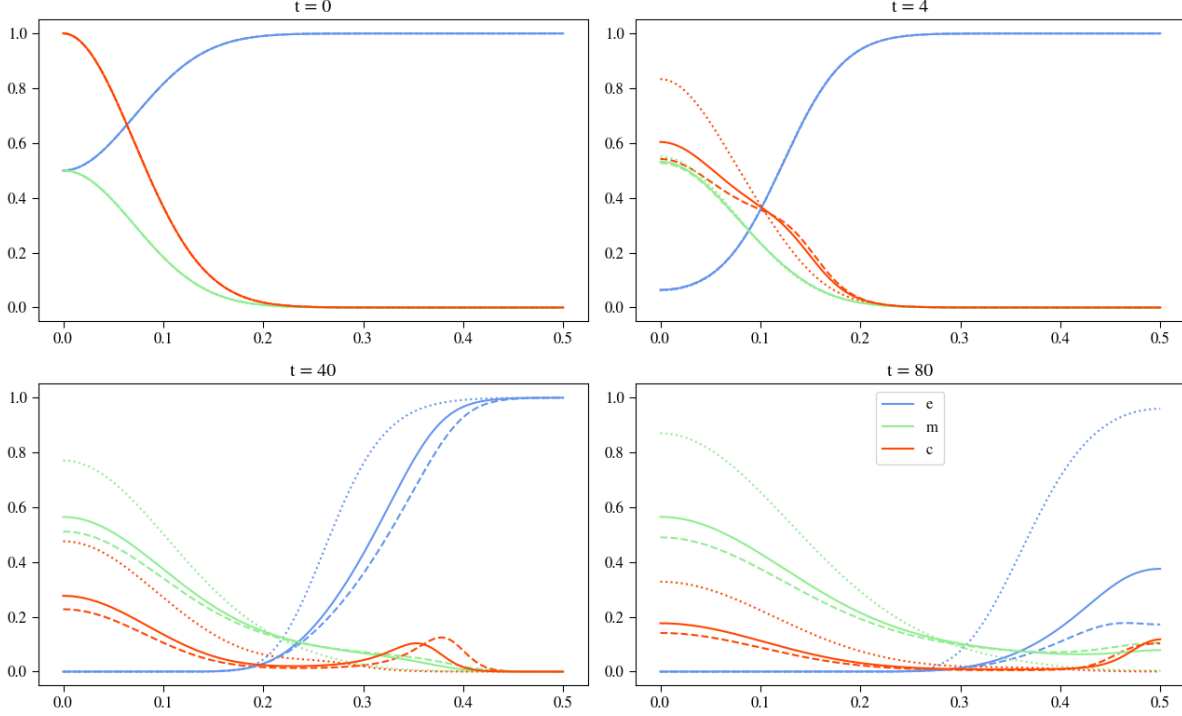


Figure 6: Plots show results for varying  $\gamma$  whilst keeping the other parameters constant, in the images you can see the effects of  $\gamma = 0.01$  in the dashed curve,  $\gamma = 0.002$  in the dotted curve and  $\gamma = 0.008$  in the solid line.

that it is still highest at the origin for the curves of  $c$  that have lower values for  $\gamma$ , this only makes sense since the tumour cells produce the MDEs. For the ECM concentration we see similar behaviour as for the MDEs, with increasing  $\gamma$ , the ECM is also faster decayed, again this also makes sense, since for higher values the  $c$  curve curve has invaded faster and has therefore established more MDEs at farther locations away from the origin decaying the ECM. The last image at  $t = 80$  confirms the observations from the previous points in time; the higher  $\gamma$  the faster the invasion pace of the tumour cells and the MDEs and therefore the faster the degradation of the ECM. When we now take a step further and increase  $\gamma$  by one potence, to  $\gamma = 0.1$ , we can observe that the invasion pace, has gotten so high, that before finishing the simulation at  $t = 80$  the tumour cells have not only invaded completely up to the border regions but have also been pulled back towards the origin upon getting reflected at the border of the unit square and also since degradation of the ECM has not kept up with the invasion pace of the tumour cells, we are left with a situation where the tumour cells have spread further than the ECM and are now being pulled back inwards toward the origin again, this can be seen in figure 7. After already  $t = 20$  the tumour cells shown on the left side in this figure they have almost reached the border, looking at the ECM at this point in time we see that the highest concentration is now in the corners of the unit square. so this is where the haptotaxis is going to pull the tumour cells, this behaviour is not anymore radially symmetrical. We see in the next point in time at  $t = 30$  that the tumour cells do exactly this moving into the corners

of the plot. Figure 8 underlines this abandoning of radial symmetry, on the left side we see the plot over line configuration we used until now, the left side shows a plot over line configuration from the origin to one of the corner. After  $t = 20$  the images on left side imply that the tumour cells get slowly pulled back in after being reflected on the border, yet with a lower density, on the right side we see that tumour cells are still getting pushed outwards into regions where there is still the most ECM. In figure ?? you can see the plot over line results using this alternative configuration. Up until  $t = 20$  everything looks like in the normal plot over line results. After this keeps going until hitting the border and getting reflected at  $x = 0.7$  which is reached between the latter two points in time. Upon getting reflected you can also see that the concentration along this line increases visibly, this is due to the tumour cells moving into the corners that have reached their borders earlier in time. As you can see this also influences the MDE and ECM concentration, with curves that are not monotone since they could keep up the pace of the tumour cells invasion speed. Whilst the ECM in regions at  $x = 0.25$  have not decayed at  $t = 60$  they form a single maxima at this point, the MDEs that have been produced at the origin are at this point in time are at the same point  $x = 0.25$  joined by the MDEs coming from the border regions where the tumour cells there have produced them. Where in all of the other experiments for varying  $\gamma$  the tumour cells invaded at such a pace, that the produced MDE concentration in their wake was sufficiently high to degrade the ECMs to not pull the tumour cells back to the remaining ECMs later and produce monotone results for both ECM and MDE concentration. Though the intuition is met that with increasing  $\gamma$  the invasion pace of the tumour cells and matrix decaying enzymes also rises, we get unexpected behaviour with the tumour cells invasion being so fast that they get reflected at the border of the unit cube and pulled into the corners and from there back in by not decayed ECM. Further increasing  $\gamma$  will only increase this behaviour and make this oscillating process even faster.

## $\eta$ Variation

The parameter  $\eta$  influences the degrading of the ECM, which happens faster for higher  $\eta$  coefficients in regions where both MDE and ECM concentration are high. Varying this parameter may have a high impact on curves for  $c$  as well, because the gradient of the ECM is a deciding factor for the effects of haptotaxis on the tumour cells, thus increasing the degradation may cause a faster shift of the ECM outwards, therefore also pulling the tumour cells faster farther out, which in turn will affect also the MDE curve.

Inspecting the images in figure 10 we see those assumptions met. The first experiment in figure 10 shows that if  $\eta = 0$ , which means that the ECM is not degraded by the MDEs, we get completely different results comparing it to the base case. Not only does  $\eta$  influence the curve for the ECM  $e$  but has also a high impact on both tumour cell density and MDE concentration. Due that no degrading happens  $e$  stays constant all the time, with  $\frac{\partial e}{\partial t} = 0$ , this also means that  $\nabla e$  stays also constant, we see this effect in the images, showing that  $c$  does not invade further than the point where  $\nabla e$  is highest, this implies that if  $c$  converges towards this point it will also have its maximum at this point, which also fixes the point  $c\nabla e$ , what does this mean for the MDEs? After initially increasing slightly around the point  $x = 0$  and increasing where  $c$  was high previously,

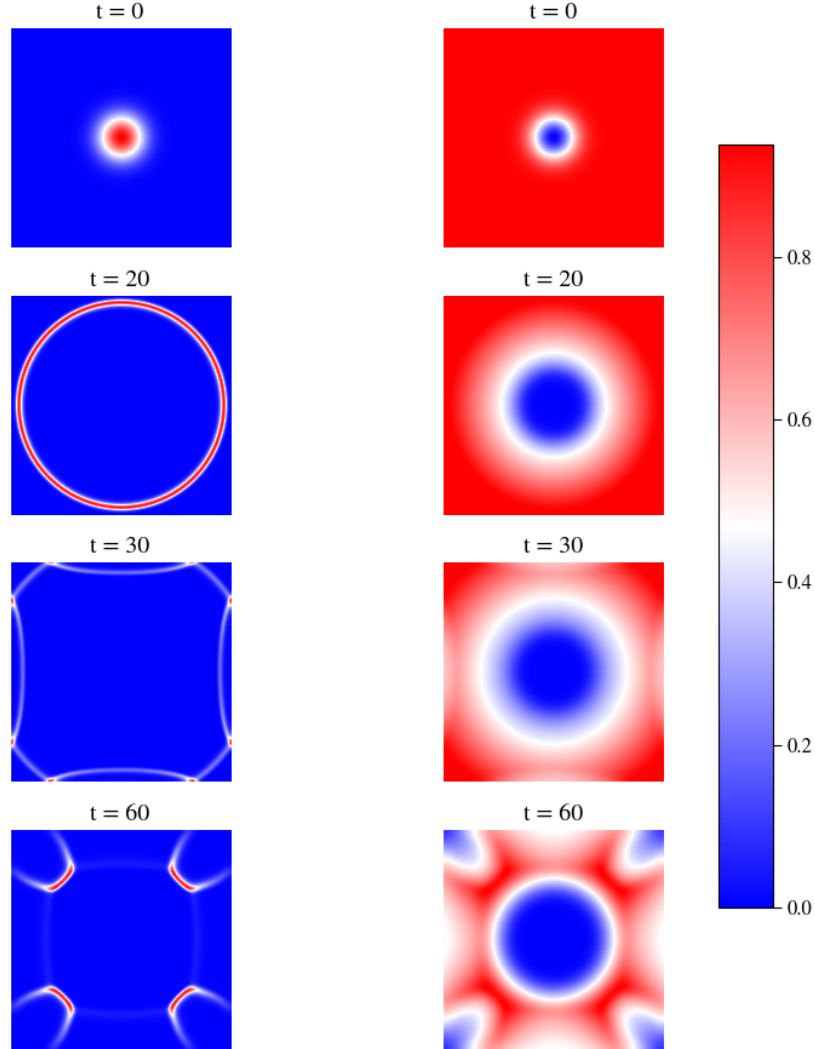


Figure 7: 2D plot of variation

it also converges with its highest concentration at  $c\nabla e$ . Since the motility of  $c$  is highly restricted due to no degradation of the ECM, the MDEs will progress to increase  $c$  takes on values higher than 0. If this simulation for  $\eta = 0$  will be continued we will see that the MDEs  $m$  will also a curve that is not monotone decreasing. Increasing  $\eta$  to  $\eta = 20$  the behaviour change is not so drastically comparing it to the base case. The degradation of the ECM happens twice as fast, which results in a faster invasion pace of the tumour cells, though with decreased influence of haptotaxis, making the hill at the leading edge smaller. After dimensionless time  $t = 8$  the ECMs have degrading has visibly increased, but the MDE concentration is still higher. This only makes sense since, needing a lower concentration to degrade the ECM, this process happens faster, and also since haptotactic influences are lower the concentration of tumour cells at the origin is higher, which will also produce more MDEs at the origin.  $\eta$  has a strong influence on all curves, if its value is lower the degradation of  $e$  happens slower, slowing also  $c$  and  $m$ 's invasion pace down.



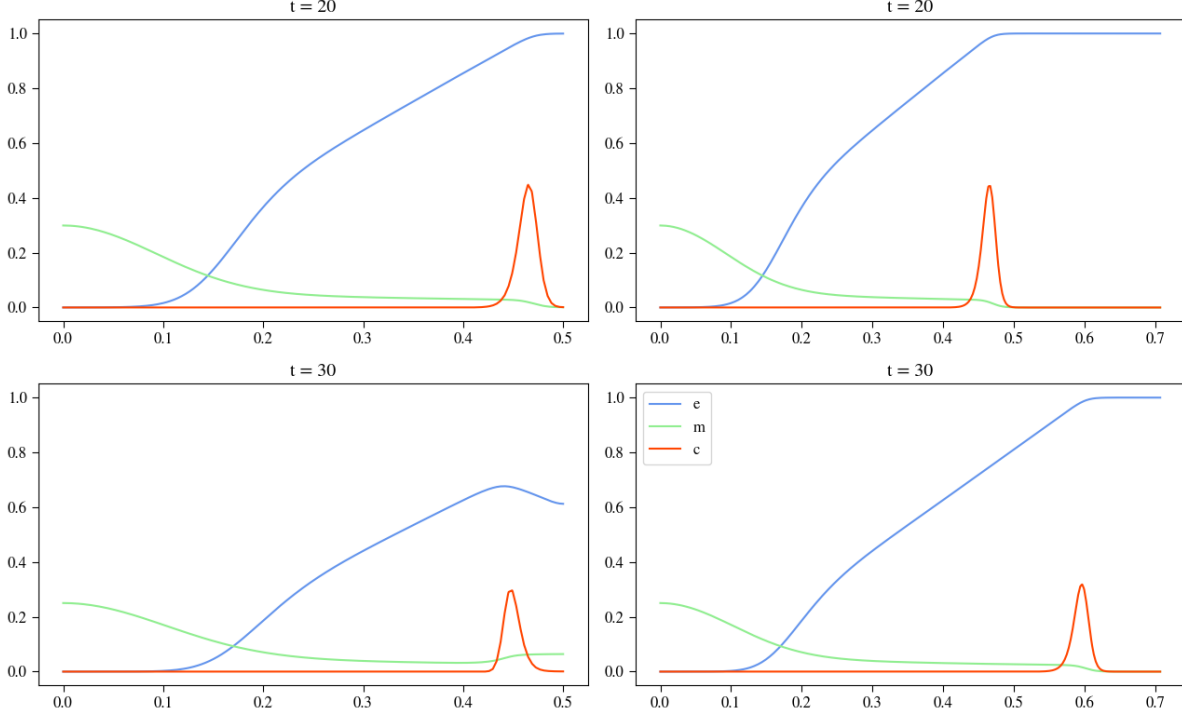


Figure 8: Plot Over Line Comparison Gamma

### $d_m$ Variation

$d_m$  is the parameter describing the diffusion of the matrix degrading enzymes MDEs, it is influenced by the second derivative of  $c$ . Looking at the equations we can expect with higher values for  $d_m$  a faster degradation of  $e$ , since the MDEs can invade faster into the space and there are not too much MDEs needed to degrade  $e$ . This will then cause a faster invasion pace of  $c$ , because the haptotatic flux pulls heavier outward. Setting  $d_m$  to zero, so no movement of the MDEs, we see that the curve still changes, which is due to the tumour cells producing them where they are. We see that the value for  $m$  around the origin is higher than 1 which is possible since their concentration could be so high that there are more than one MDE per mesh point, although this would require to make the mesh finer I think. If we look in the other direction, setting  $d_m$  to  $1e-1 = 0.1$  we see that after already  $t = 0.4$  the MDEs have spread completely throughout space, from this point on, they are mostly subject to the production term yielded by the tumour cells, but as fast as they are produced, so fast they are also distributed in space, causing a seemingly equilibrium throughout space for the MDE concentration regardless of the local tumour cell density. As we saw earlier a low concentration for MDEs is needed to efficiently degrade the ECM, therefore degradation happens a lot faster here, even so fast, that the gradient of  $e$  diminishes as fast that the haptotatic influences of the tumour cells are reduced, causing tumour spread to slow down. This is contrary to our initial assumption that with higher values for  $d_m$  the tumour invasion pace will also increase. This parameter therefore seems to have influence on the haptotatic effects and the overall

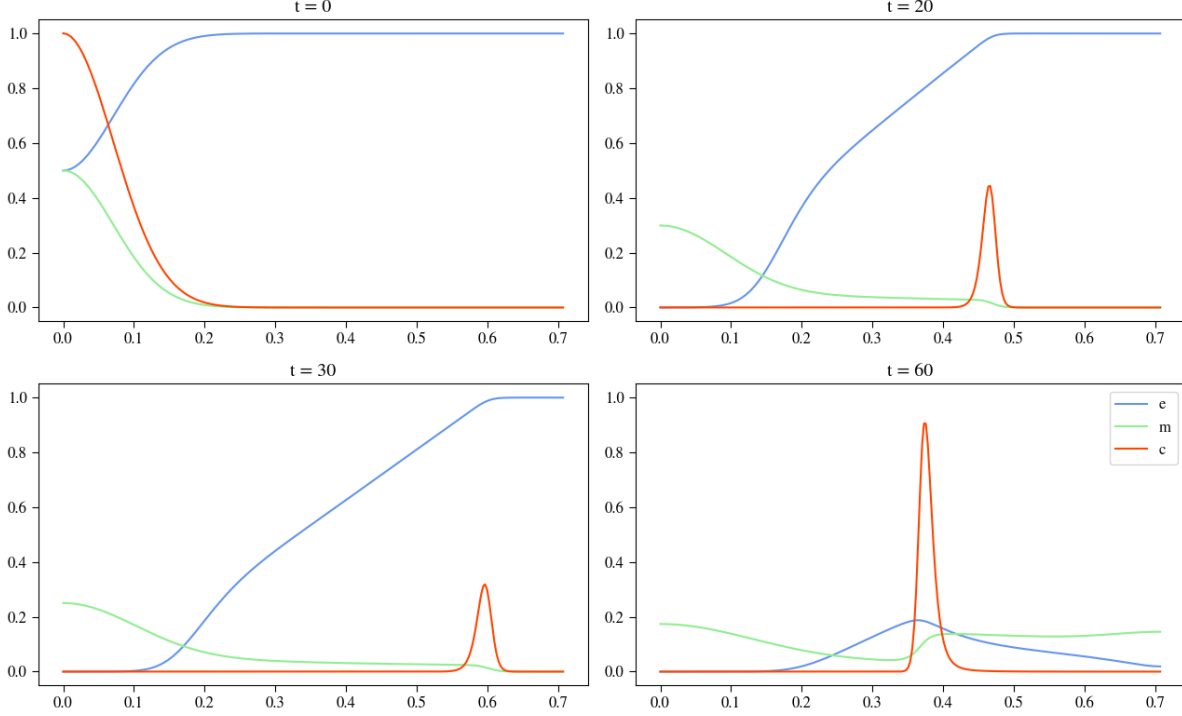


Figure 9: gamma alternative plot over line

extra cellular matrix degradation.

### $\alpha$ Variation

When we look at  $\alpha$  in a range from 0.0 to 1.0 we can expect with growing  $\alpha$  a faster degrading of the ECM and higher values form the MDEs themselves. Faster ECM degrading could mean fast invasion of the tissue of the tumour cells. As we saw in the previous comparison, the MDEs can take on values higher than one, we can also expect this here when  $\alpha$  is sufficiently high. Looking at the experiment with  $\alpha = 0.0$  we can see that at the end the ECM has still much higher values than compared with the baseline experiment at dimensionless time  $t = 8$  and as expected the invasion pace of the tumour cells is considerably slower. Comparing this to the plots for  $\alpha = 1.0$  we can see that after already  $t = 4$  the MDEs have taken on a contraction of greater than one at  $x = 0$ . Overall is the degradation happening faster and therefore also the tumour invasion happens faster. In the end we are left with a clearly lower ECM concentration than for example the baseline experiment.

### $\beta$ Variation

Looking at  $\beta$  which is the parameter describing decay of the MDEs, we can assume that with varying  $\beta$  the MDE curve will be lower, influencing the ECM degrading process and therefore also the invasion pace. Since all previous experiments assumed a value of  $\beta = 0$

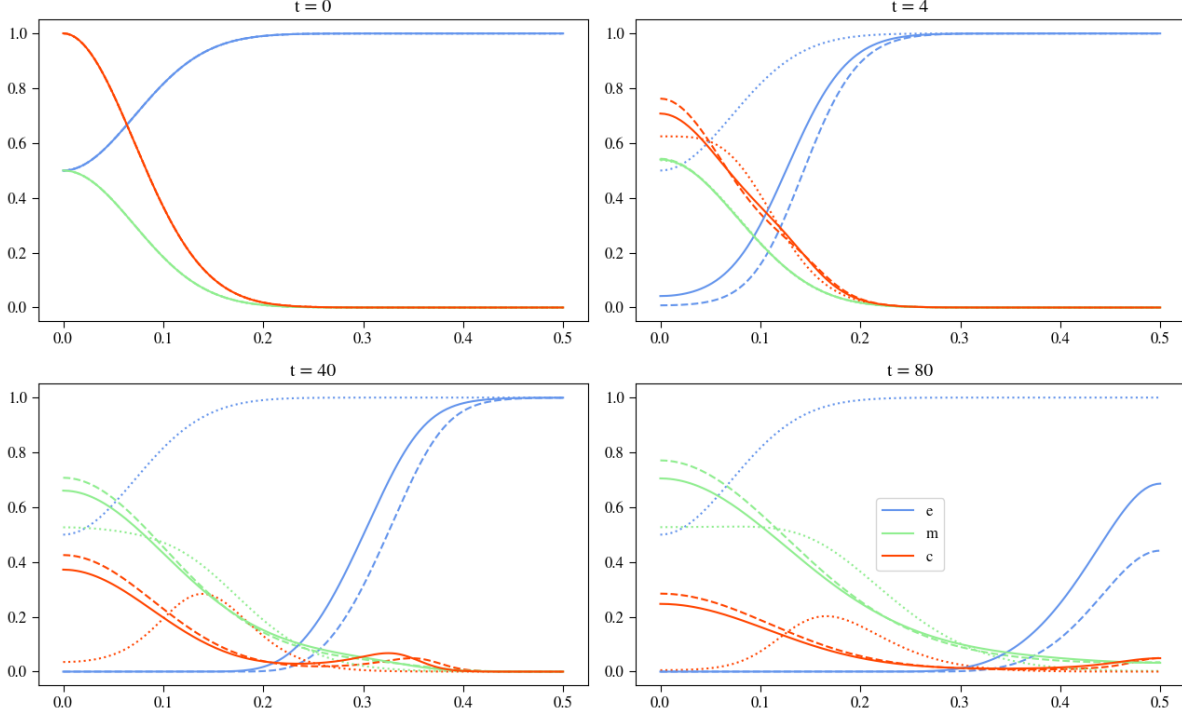


Figure 10: Plots show results for varying  $\eta$  whilst keeping the other parameters constant, in the images you can see the effects of  $\eta = 20$  in the dashed curve,  $\eta = 0$  in the dotted curve and  $\eta = 12$  in the solid line.

we can expect that with growing  $\beta$  these effects will increase continuously. We first of all needed to determine a range in which to experiment. Starting with a range of values between 0.1 and 1.0, since this is the range  $\alpha$  yields reasonable results we saw that those values were much too high. Even for  $\beta = 0.1$  the MDEs are almost completely decayed after only  $t = 0.4$ , looking closer at ParaView this happened after already  $t = 0.1$ . This also affects the haptotactic effects of the tumour cell invasion, having no secession formed at the leading edge of the tumour cells. Reducing the range for  $\beta$  one potence we can see the same behaviour, with a fast decay of the MDEs therefore lower ECM degrading and slower invasion pace. Yet looking at  $\beta = 0.01$  we see the effects of haptotaxis now again and the ECM degrading happens here visibly faster, though the MDE concentration is generally lower. This lead us to decrease  $\beta$  even further. Though if we look at  $\beta = 0.001$  we see that the effects of  $\beta$  are barely recognizable anymore. Taking the middle of those and setting  $\beta$  to 0.005, we see all the presumed effects of slowed degradation of the ECM therefore also slowed invasion pace, yet still having the effects of haptotaxis also clearly visible.

### Cross Variation

Having done all those experiments it will be interesting to compare countering effects and supporting effects two at a time

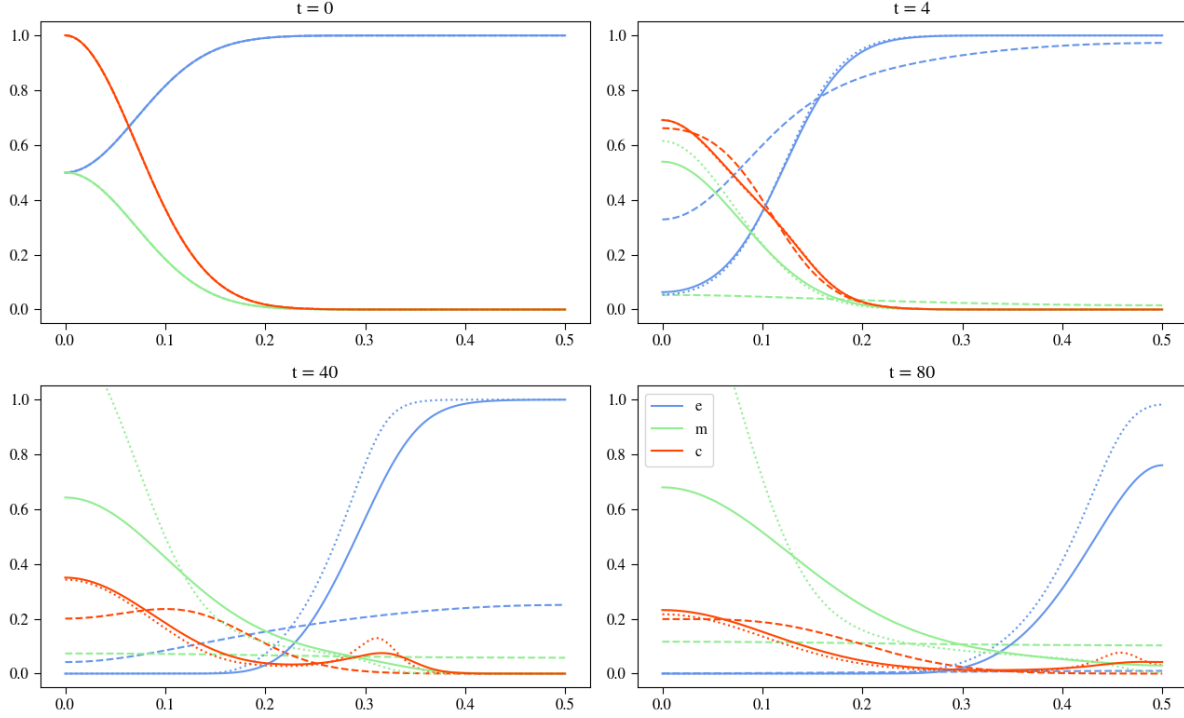


Figure 11: Plots show results for varying  $d_m$  whilst keeping the other parameters constant, in the images you can see the effects of  $d_m = 1e - 1 = 0.1$  in the dashed curve,  $d_m = 0$  in the dotted curve and  $d_m = 1e - 3 = 0.001$  in the solid line.

## 5.2 Two dimensional Results with Proliferation

## 5.3 Three Dimensional Results

### 5.3.1 Replicating Results

### 5.3.2 Parameter Analysis

## 5.4 Three Dimensional Simulations with Heterogenous ECM Structure

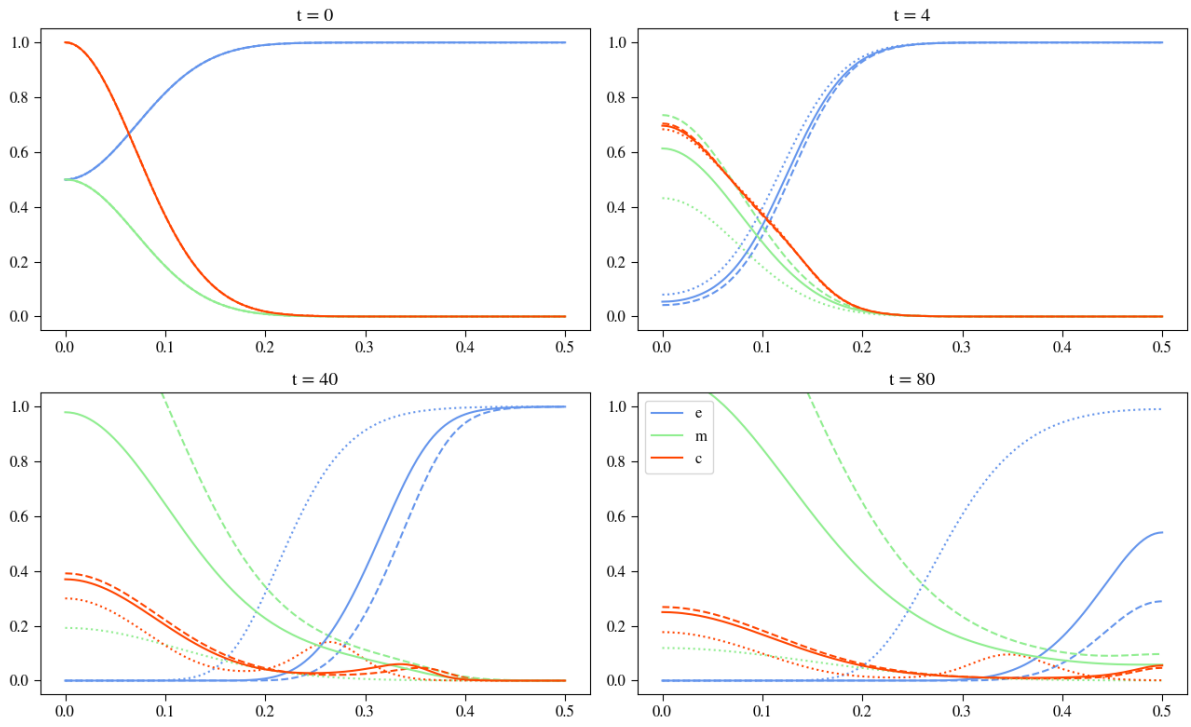


Figure 12: Plots show results for varying  $\alpha$  whilst keeping the other parameters constant, in the images you can see the effects of  $\alpha = 1.0$  in the dashed curve,  $\alpha = 0$  in the dotted curve and  $\alpha = 0.6$  in the solid line.

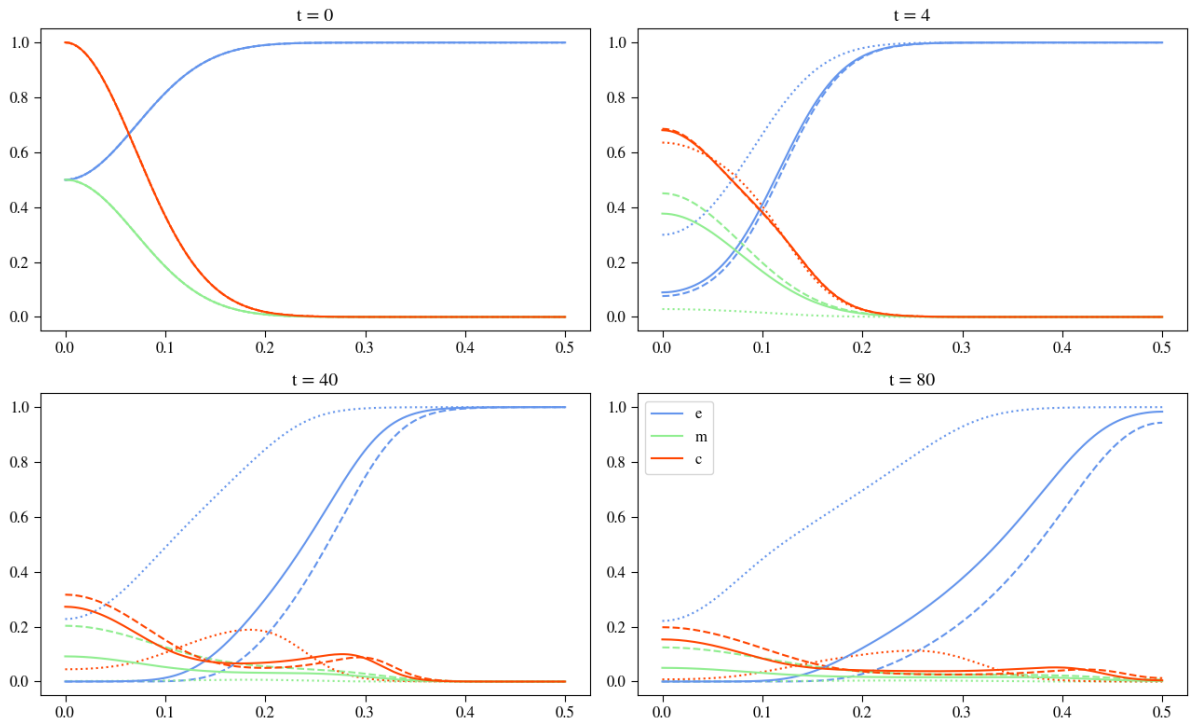


Figure 13: Plots show results for varying  $\beta$  whilst keeping the other parameters constant, in the images you can see the effects of  $\beta = 0.005$  in the dashed curve,  $\beta = 0.1$  in the dotted curve and  $\beta = 0.01$  in the solid line.

## **6 Conclusion and Discussion**

### **6.1 Extra-Dimension Evaluation**

Ergebnisse reporuzieren und vergleichen.

### **6.2 Inter-Dimension Evaluation**

## References

1. Anderson, A. Continuous and Discrete Mathematical Models of Tumor-induced Angiogenesis. en. *Bulletin of Mathematical Biology* **60**, 857–899. ISSN: 00928240. <http://link.springer.com/10.1006/bulm.1998.0042> (2023) (Sept. 1998).
2. Anderson, A. R. A., Chaplain, M. A. J., Newman, E. L., Steele, R. J. C. & Thompson, A. M. Mathematical Modelling of Tumour Invasion and Metastasis. en. *Journal of Theoretical Medicine* **2**, 129–154. ISSN: 1027-3662, 1607-8578. <http://www.hindawi.com/journals/cmmm/2000/490902/abs/> (2023) (2000).
3. Franssen, L. C., Lorenzi, T., Burgess, A. E. F. & Chaplain, M. A. J. A Mathematical Framework for Modelling the Metastatic Spread of Cancer. en. *Bulletin of Mathematical Biology* **81**, 1965–2010. ISSN: 0092-8240, 1522-9602. <http://link.springer.com/10.1007/s11538-019-00597-x> (2023) (June 2019).
4. Chaplain, M., Lolas, G. & ,The SIMBIOS Centre, Division of Mathematics, University of Dundee, Dundee DD1 4HN. Mathematical modelling of cancer invasion of tissue: dynamic heterogeneity. en. *Networks & Heterogeneous Media* **1**, 399–439. ISSN: 1556-181X. <http://aims sciences.org//article/doi/10.3934/nhm.2006.1.399> (2023) (2006).
5. Chaplain, M., McDougall, S. & Anderson, A. MATHEMATIC@ArticleKolev2010, author=Kolev, M. and Zubik-Kowal, B., title=Numerical Solutions for a Model of Tissue Invasion and Migration of Tumour Cells, journal=Computational and Mathematical Methods in Medicine, year=2010, month=Dec, day=30, publisher=Hindawi Publishing Corporation, volume=2011, pages=452320, abstract=The goal of this paper is to construct a new algorithm for the numerical simulations of the evolution of tumour invasion and metastasis. By means of mathematical model equations and their numerical solutions we investigate how cancer cells can produce and secrete matrixdegradative enzymes, degrade extracellular matrix, and invade due to diffusion and haptotactic migration. For the numerical simulations of the interactions between the tumour cells and the surrounding tissue, we apply numerical approximations, which are spectrally accurate and based on small amounts of grid-points. Our numerical experiments illustrate the metastatic ability of tumour cells.,@article10.14492/hokmj/1520928060, author = Akio ITO, title = Large-time behavior of solutions to a tumor invasion model of Chaplain–Anderson type with quasi-variational structure, volume = 47, journal = Hokkaido Mathematical Journal, number = 1, publisher = Hokkaido University, Department of Mathematics, pages = 33 – 67, keywords = large-time behavior, quasi-variational structure, tumor invasion, year = 2018, doi = 10.14492/hokmj/1520928060, URL = <https://doi.org/10.14492/hokmj/1520928060> doi=10.1155/2011/452320, url=<https://doi.org/10.1155/2011/452320> AL MODELING OF TUMOR-INDUCED ANGIOGENESIS. en. *Annual Review of Biomedical Engineering* **8**, 233–257. ISSN: 1523-9829, 1545-4274. <https://www.annualreviews.org/doi/10.1146/annurev.bioeng.8.061505.095807> (2023) (Aug. 2006).



6. Kolev, M. & Zubik-Kowal, B. Numerical Solutions for a Model of Tissue Invasion and Migration of Tumour Cells. *Computational and Mathematical Methods in Medicine* **2011**, 452320. ISSN: 1748-670X. <https://doi.org/10.1155/2011/452320> (Dec. 2010).